Urbanization-induced warming amplifies population exposure to compound heatwaves but narrows exposure inequality between global North and South cities

Shengjun Gao [1, 2], Yunhao Chen [1, 2, *], Deliang Chen [3], Bin He [4], Adu Gong [1, 2, 5], Peng Hou [6], Kangning Li [7], Ying Cui [1, 2]

1 State Key Laboratory of Remote Sensing Science, Faculty of Geographical Science, Beijing Normal University, Beijing 100875, China

2 Beijing Key Laboratory of Environmental Remote Sensing and Digital Cities, Faculty of Geographical Science, Beijing Normal University, Beijing 100875, China

3 Regional Climate Group, Department of Earth Sciences, University of Gothenburg, Gothenburg, S-40530, Sweden

4 State Key Laboratory of Earth Surface Processes and Resource Ecology, Faculty of Geographical Science, Beijing Normal University, Beijing 100875, China

5 Beijing Engineering Research Center for Global Land Remote Sensing Products, Faculty of Geographical Science, Beijing Normal University, Beijing 100875, China

6 Satellite Environment Center, Ministry of Ecology and Environment, Beijing 100094, China

7 College of Geoscience and Surveying Engineering, China University of Mining and Technology-Beijing, Beijing 100083, China

Corresponding author: Yunhao Chen

E-mail: cyh@bnu.edu.cn

Supplementary Discussion

We explored the impact of urbanization-induced warming on urban heat exposure. Urbanization-induced warming (i.e. the difference of compound heatwaves between urban and rural) was calculated based on gridded near-surface air temperature data [1]. To verify the validity of gridded near-surface air temperature data in the study, we compared urbanization-induced warming calculated from gridded data and weather station data. We got over 40,000 weather sites from Global Historical Climatology Network daily (GHCN daily) and China Meteorological Data Service Center. First, we excluded sites where the number of missing values for daily maximum and minimum temperatures was more than 30 days during the extended summer period from 2003 to 2019. And the average of the two days before and after the missing values were used to interpolate missing values. Also, we chose cities with at least one site in both urban and rural areas and ended up with 86 cities.

Our study of the effects of urbanization-induced warming on heat exposure was not a comparison between individual cities, but a comparison between cities in the global North and South, and this regional averaging reduced uncertainty [2]. We compared the urbanization-induced increase in compound heatwaves between cities in the global South (number of cities: 35) and global North (number of cities: 51). As shown in Supplementary Fig. 13, We found that the urbanization-induced warming based on site data was consistent with the grid data, that is, the urbanization-induced warming was stronger in the global North cities than in the global South cities. Moreover, the regional disparities of urban-rural heatwave differences showed consistency in both gridded dataset and station observations. For example, cumulative heat, which is main used heatwave indicator, differed between the global North and South by 3.69 and 3.97 in the gridded dataset and station observations, respectively (Supplementary Fig. 13d). Finally, we also repeated our experimental using remotely sensed temperatures [3]. We found that urbanization-induced warming was stronger in the global North based on extreme land surface temperatures (Supplementary Fig. 14a), and that the disparity in heat exposure between the global South and North would be overestimated when urban warming was not considered (Supplementary Fig. 14b). This was consistent with our findings using air temperature. The above analysis indicated the reliability of current results.

Supplementary Figures

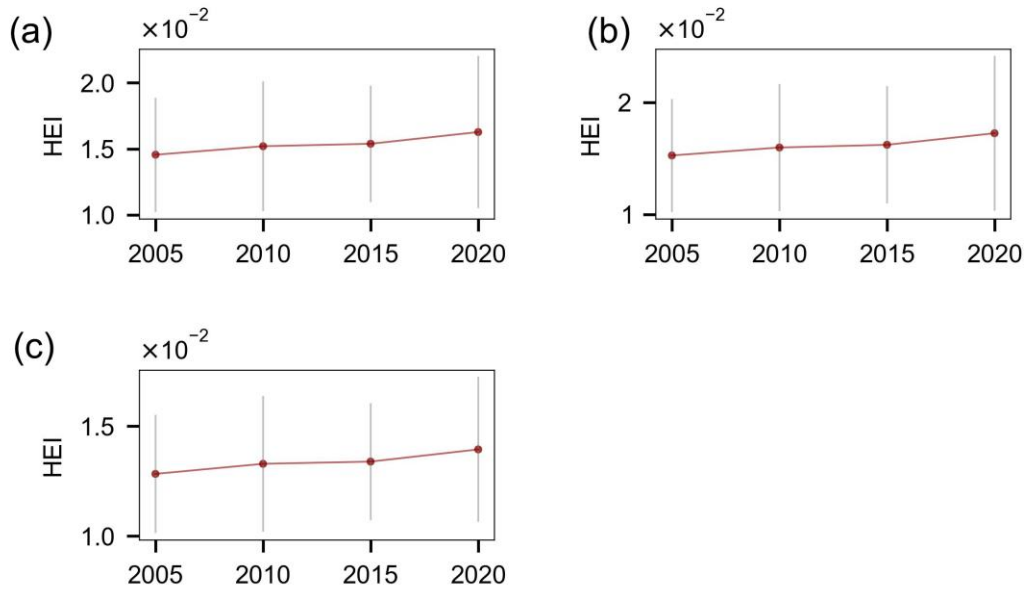

Supplementary Fig. 1. Temporal changes of heat exposure in urban areas (a), high urbanization areas (b), and low urbanization areas (c). Dots indicate mean values and gray line indicate standard deviations.

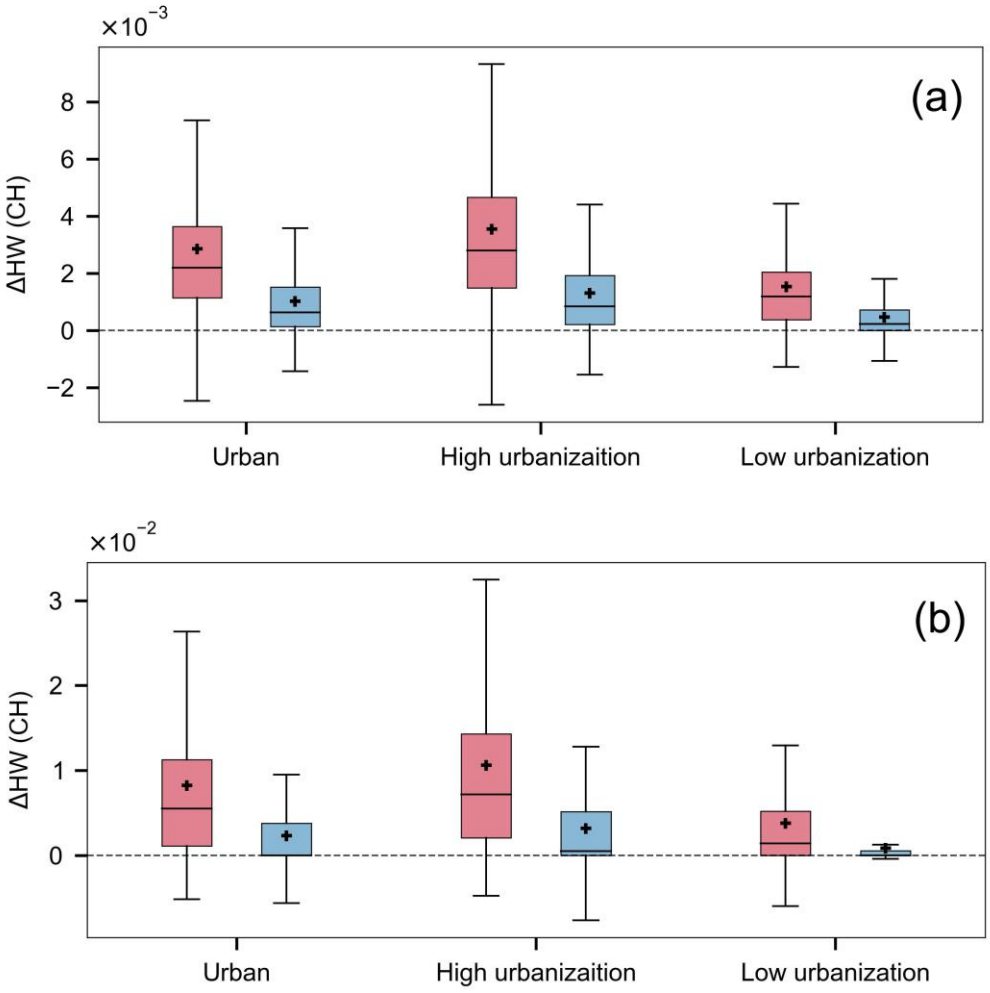

Supplementary Fig. 2. Urban-rural heatwave differences in Global North (red) and Global South (blue) cities. Heatwaves are defined using 95% (a) and 98% (b) temperature thresholds, respectively. The heatwave index is cumulative heat. Box plots represent the interquartile range (IQR) as the box, median as a horizontal line within the box, mean as a point within the box, and 1.5× IQR as the whiskers. Outliers are omitted for clarity.

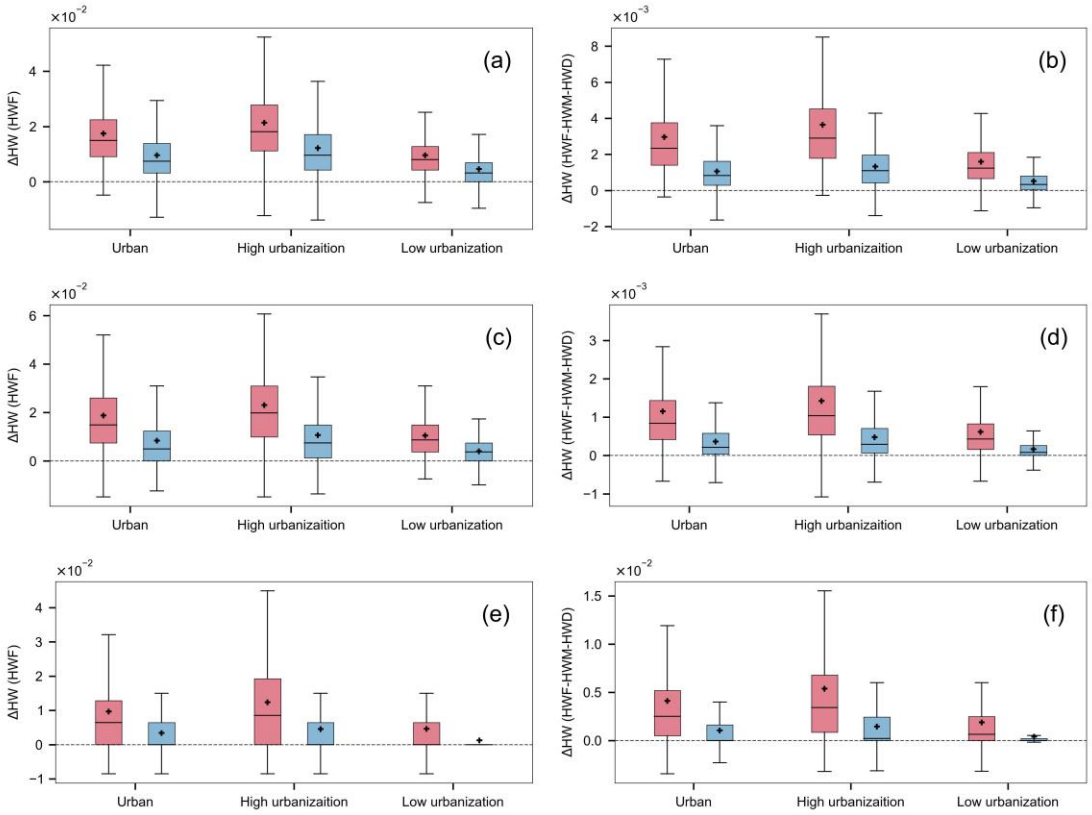

Supplementary Fig. 3. Urban-rural heatwave differences in Global North (red) and Global South (blue) cities. The heatwave indices are heatwave frequency (a, c, e) and coupled heatwave frequency, heatwave magnitude and heatwave duration (b, d, f), respectively. Heatwaves are defined using 90% (a, b), 95% (c, d), and 98% (e, f) temperature thresholds, respectively. Box plots represent the interquartile range (IQR) as the box, median as a horizontal line within the box, mean as a point within the box, and 1.5× IQR as the whiskers. Outliers are omitted for clarity.

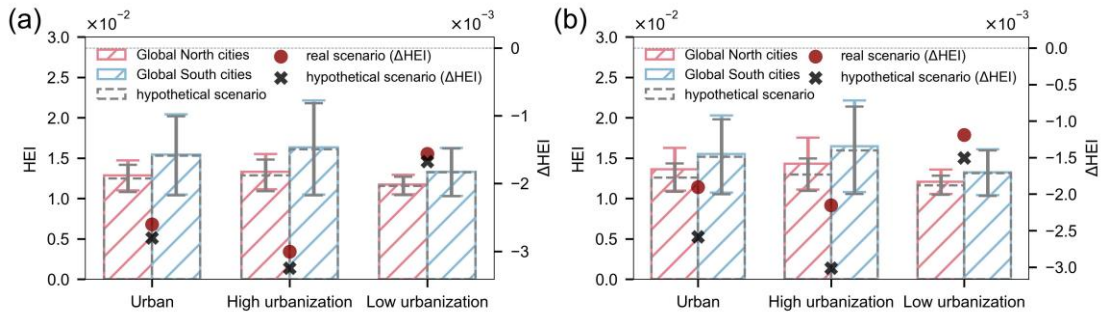

Supplementary Fig. 4. Differences in HEI between the global North and South cities. Heatwaves are defined using 95% (a) and 98% (b) temperature thresholds, respectively. The heatwave index is cumulative heat. Heat exposure levels of global North and South cities are represented in red bar graph and blue bar graph, respectively, when considering urbanization-induced warming (real scenario). Heat exposure levels of global North and South cities without considering urbanization-induced warming (hypothetical scenario) are shown in grey bar graph. Error bars indicate standard deviation. The red and black dots indicate the average HEI difference between the global North and global South cities under the real and hypothetical scenarios, respectively.

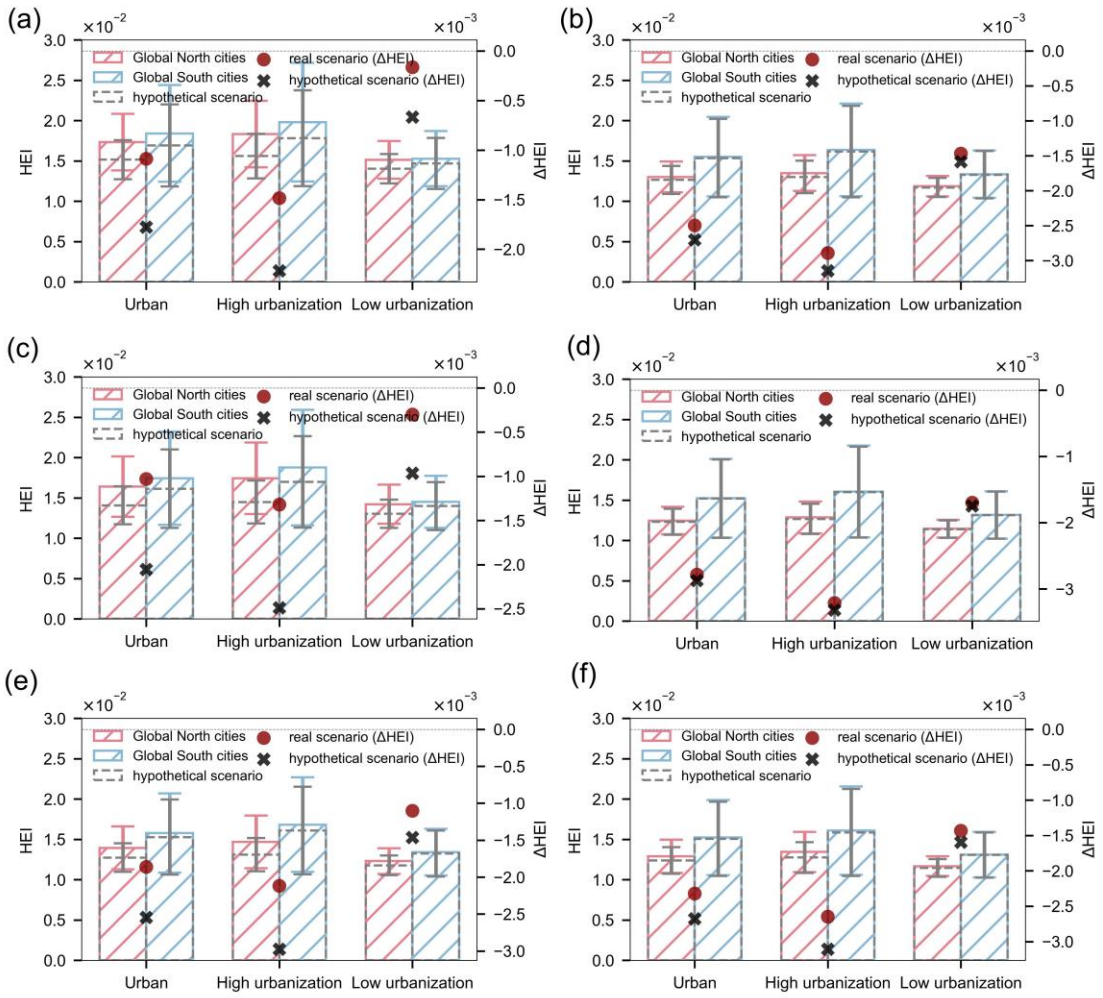

Supplementary Fig. 5. Differences in HEI between the global North and South cities. The heatwave indices are heatwave frequency (a, c, e) and coupled heatwave frequency, heatwave magnitude and heatwave duration (b, d, f), respectively. Heatwaves are defined using 90% (a, b), 95% (c, d), and 98% (e, f) temperature thresholds, respectively. Heat exposure levels of global North and South cities are represented in red bar graph and blue bar graph, respectively, when considering urbanization-induced warming (real scenario). Heat exposure levels of global North and South cities without considering urbanization-induced warming (hypothetical scenario) are shown in grey bar graph. Error bars indicate standard deviation. The red and black dots indicate the average HEI difference between the global North and global South cities under the real and hypothetical scenarios, respectively.

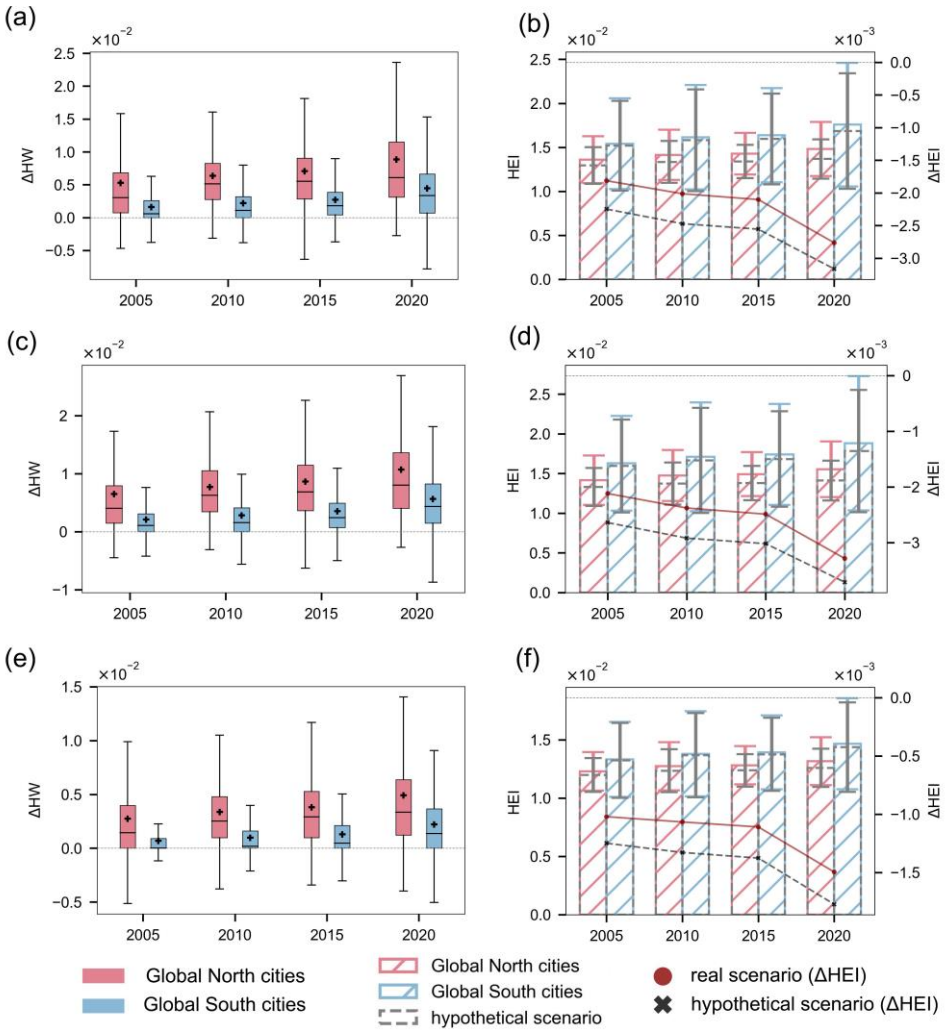

Supplementary Fig. 6. Contrasting differences of urban-rural heatwave (a, c, e) and heat exposure (b, d, f) between global North and global South cities. Urban-rural heatwave differences in urban areas (a), high urbanization areas (c), and low urbanization areas (e). Box plots represent the interquartile range (IQR) as the box, median as a horizontal line within the box, mean as a point within the box, and 1.5× IQR as the whiskers. Outliers are omitted for clarity. Urban-rural heat exposure differences in urban areas (b), high urbanization areas (d), and low urbanization areas (f). Heat exposure levels of global North and South cities are represented in red bar graph and blue bar graph, respectively, when considering urbanization-induced warming (real scenario). Heat exposure levels of global North and South cities without considering urbanization-induced warming (hypothetical scenario) are shown in grey bar graph. Error bars indicate standard deviation. The red and black dots indicate the average HEI difference between the global North and global South cities under the real and hypothetical scenarios, respectively.

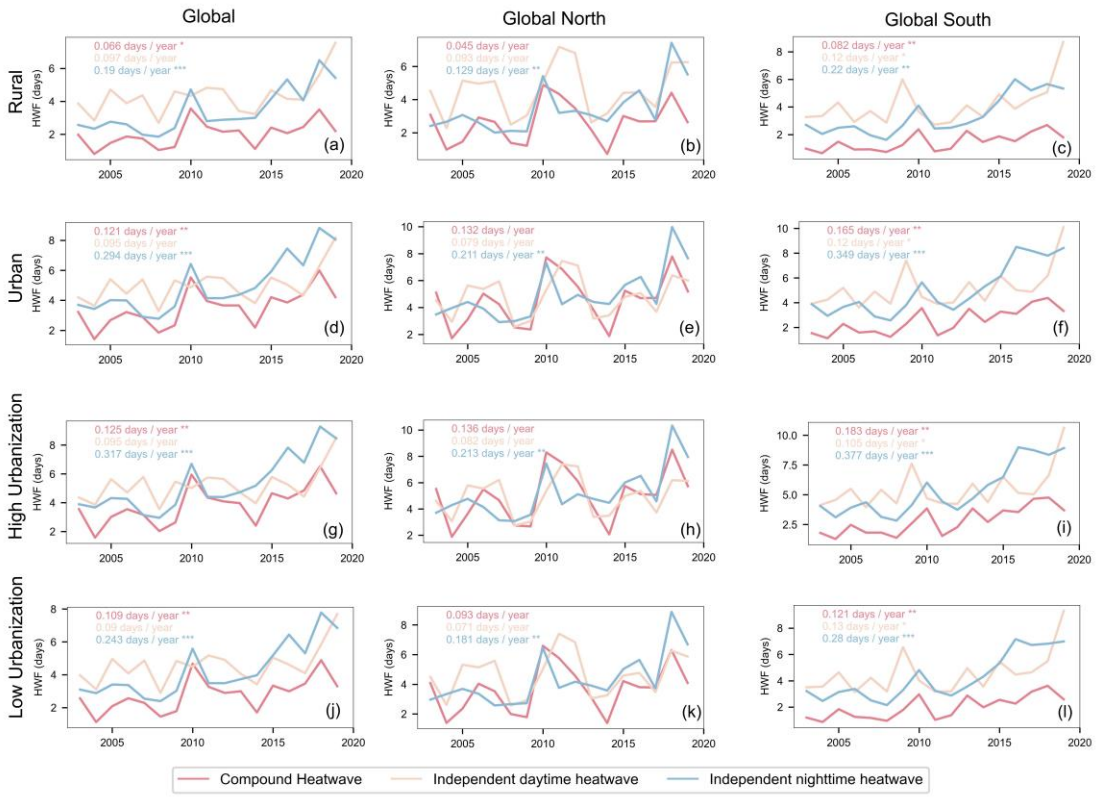

Supplementary Fig. 7. Temporal trends in heatwave frequency. The Sen's slope estimator and Mann–Kendall test were utilized to test the time trends and their significance. '*', '**' and '***' indicate significant at the 0.05, 0.01, and 0.001 levels, respectively.

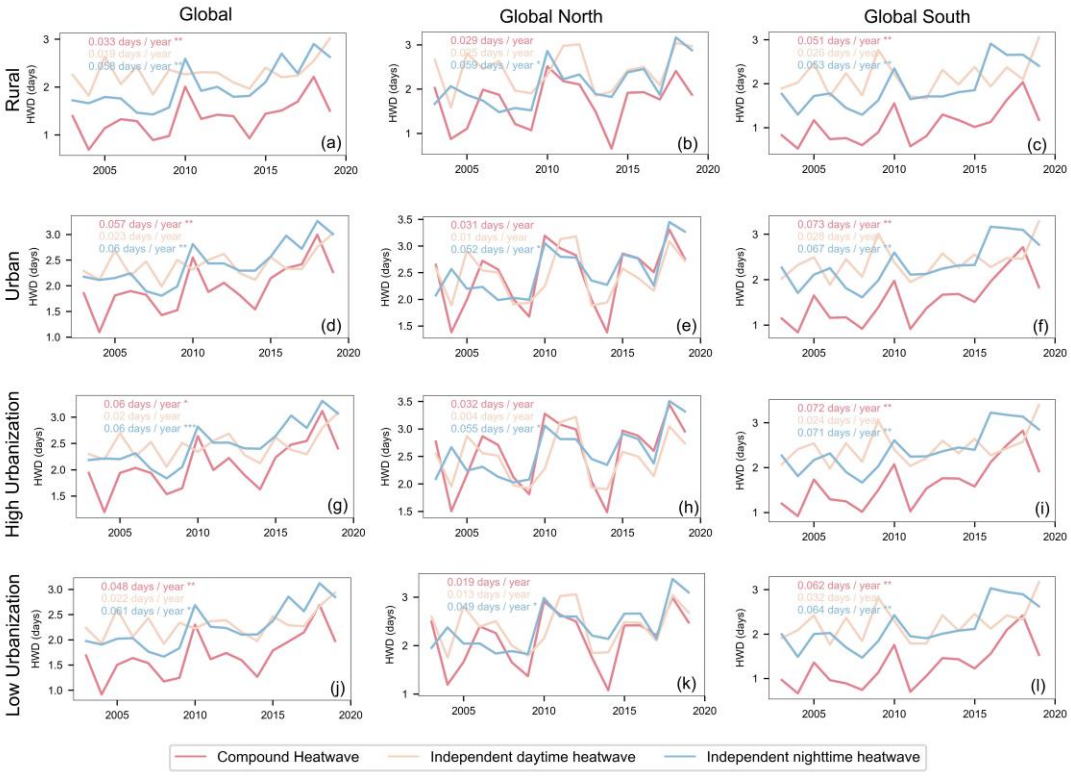

Supplementary Fig. 8. Temporal trends in heatwave duration. The Sen's slope estimator and Mann–Kendall test were utilized to test the time trends and their significance. '*', '**' and '***' indicate significant at the 0.05, 0.01, and 0.001 levels, respectively.

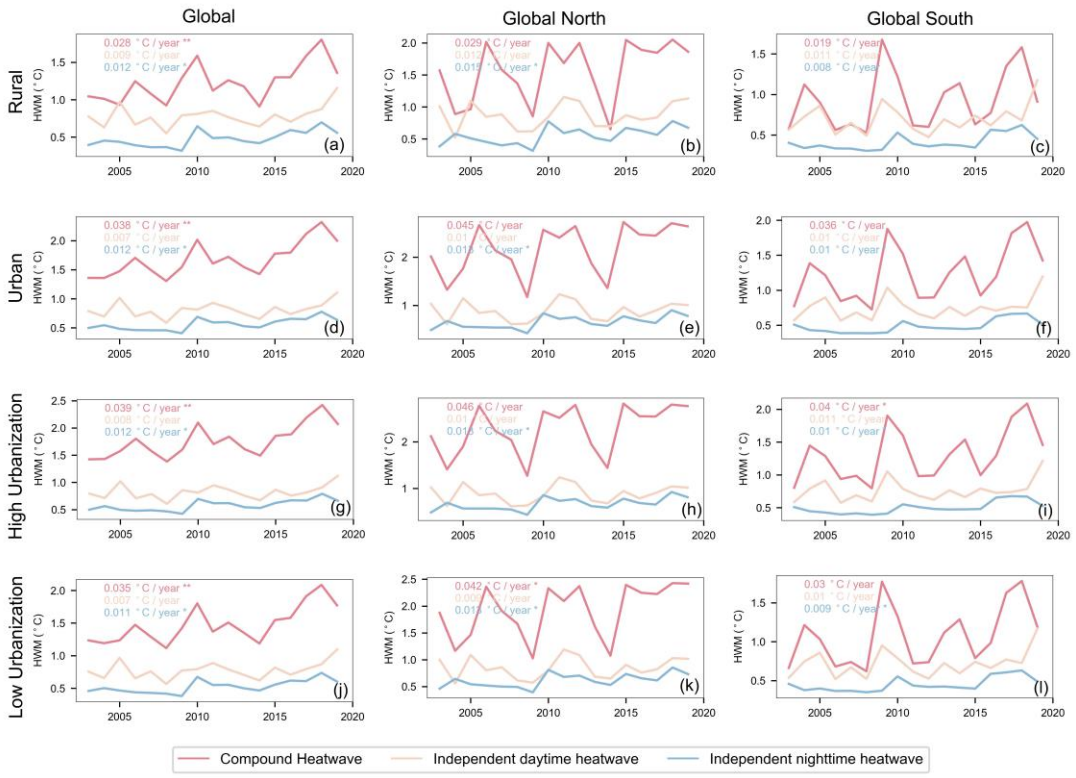

Supplementary Fig. 9. Temporal trends in heatwave magnitude. The Sen's slope estimator and Mann–Kendall test were utilized to test the time trends and their significance. '*', '**' and '***' indicate significant at the 0.05, 0.01, and 0.001 levels, respectively.

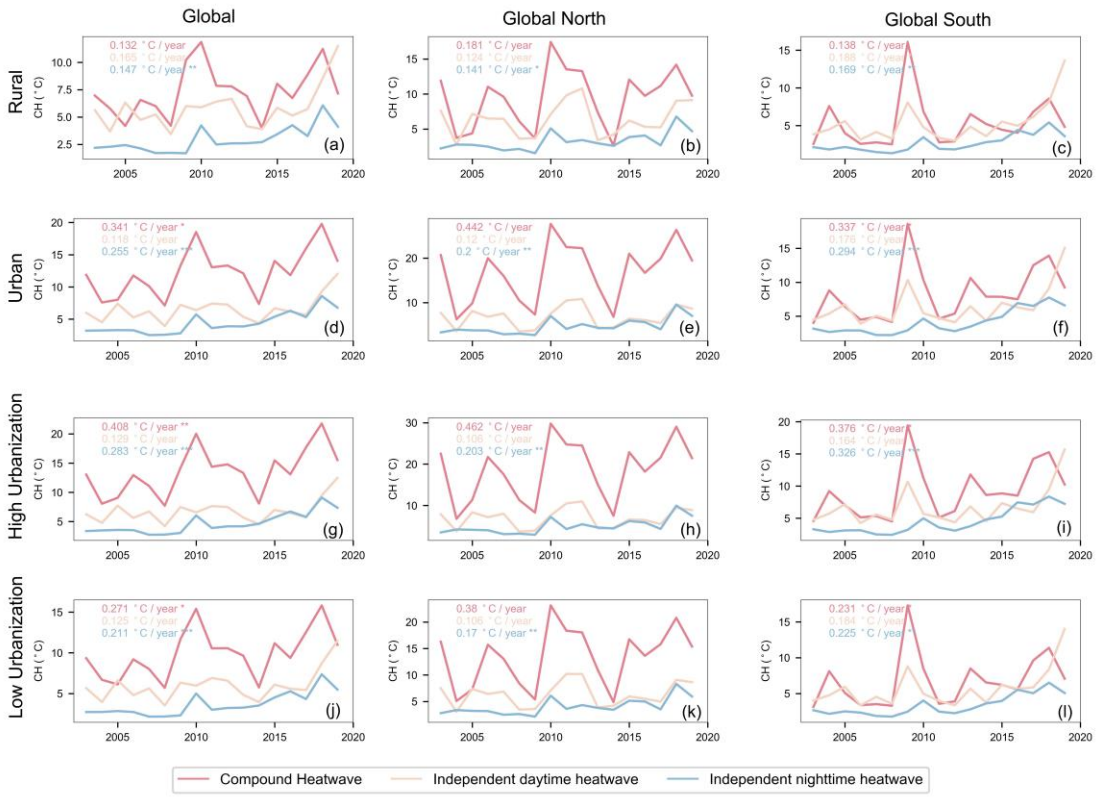

Supplementary Fig. 10. Temporal trends in cumulative heat. The Sen's slope estimator and Mann–Kendall test were utilized to test the time trends and their significance. '*', '**' and '***' indicate significant at the 0.05, 0.01, and 0.001 levels, respectively.

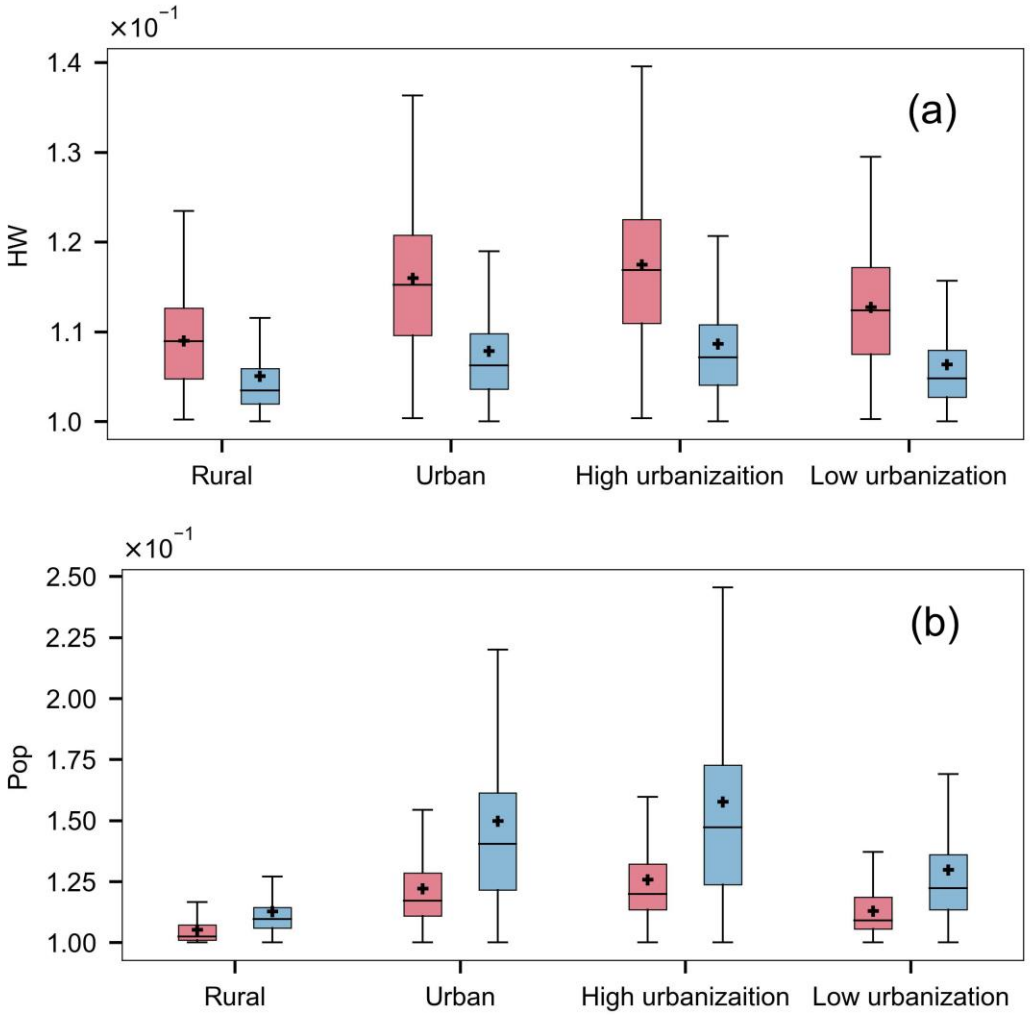

Supplementary Fig. 11. Regional statistics of heatwave index (a) and population index (b). 'Red box' represents the Global North cities and 'Blue box' represents the Global South cities. Box plots represent the interquartile range (IQR) as the box, median as a horizontal line within the box, mean as a point within the box, and 1.5× IQR as the whiskers. Outliers are omitted for clarity.

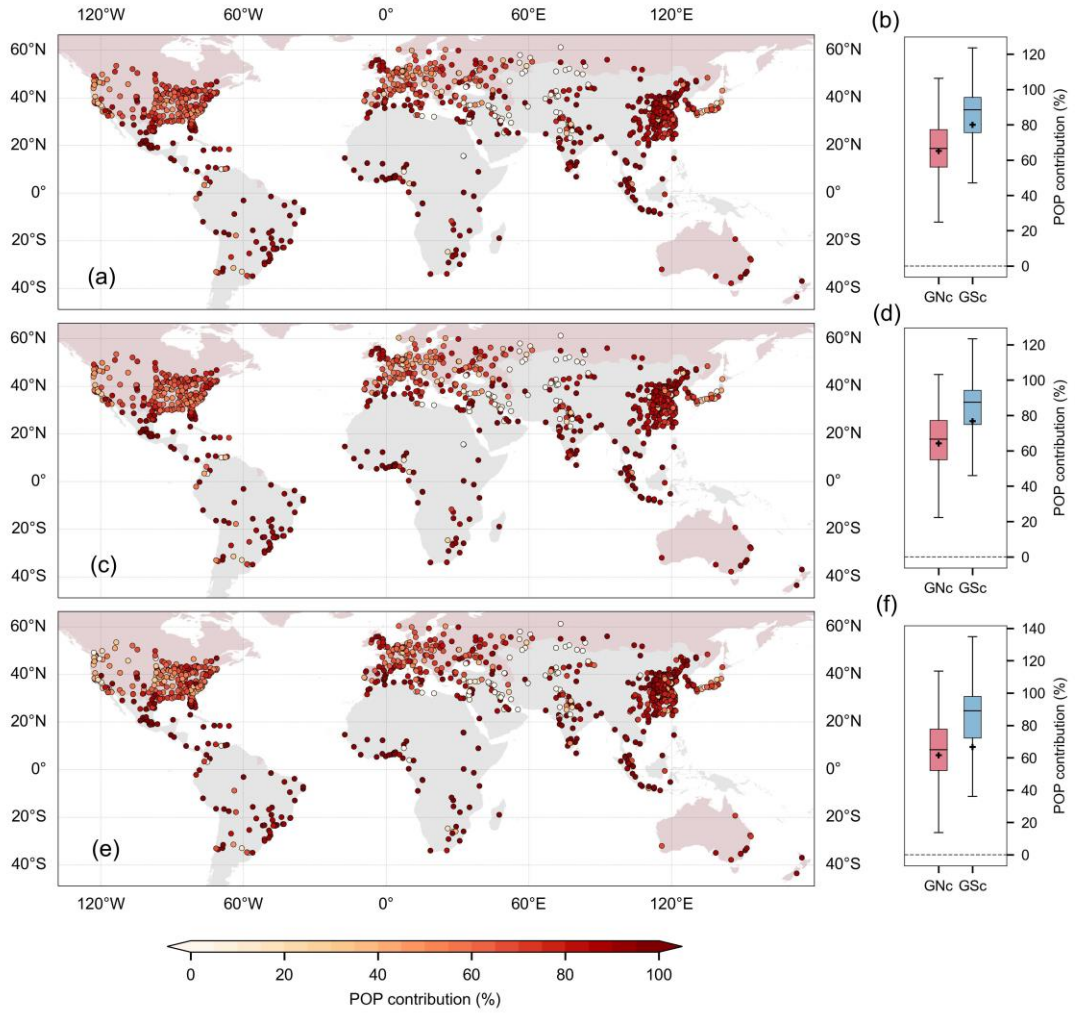

Supplementary Fig. 12. Contribution of population to the heat exposure index in urban areas (a, b), high urbanization areas (c, d), and low urbanization areas (e, f). 'GNc' represents the Global North cities and 'GSc' represents the Global South cities. Box plots represent the interquartile range (IQR) as the box, median as a horizontal line within the box, mean as a point within the box, and 1.5× IQR as the whiskers. Outliers are omitted for clarity.

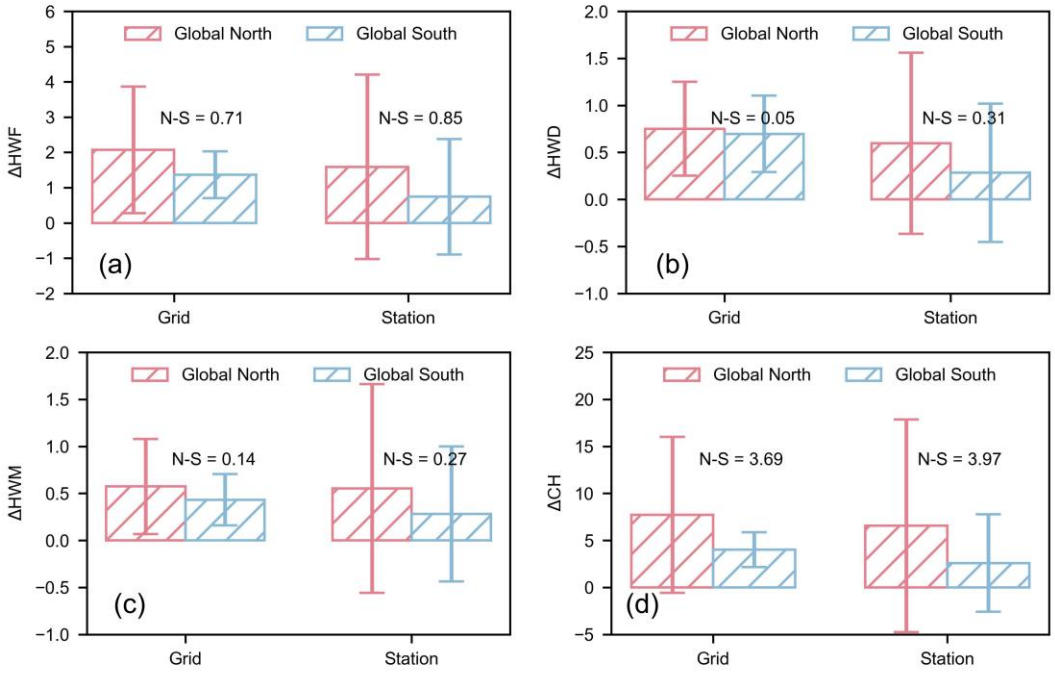

Supplementary Fig. 13. Regional statistics of urban-rural heatwave differences based on grid data and weather station data. 'Red' represents the Global North cities and 'Blue' represents the Global South cities. Error bars indicate standard deviation.

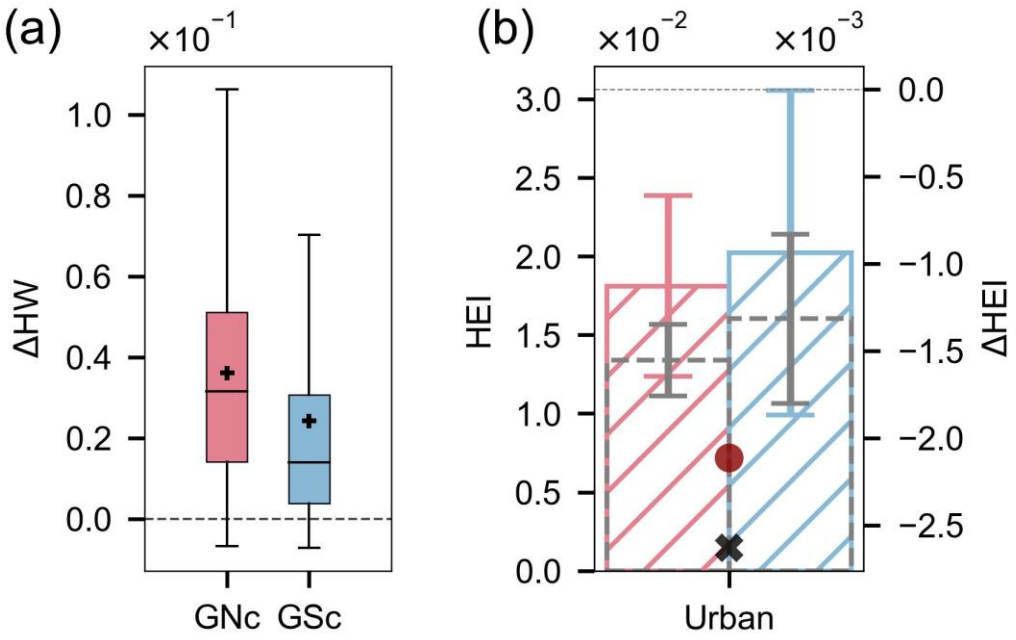

Supplementary Fig. 14. The disparity in heatwave and heat exposure between the global South and North. They are calculated based on land surface temperatures. (a) Urban-rural heatwave differences in Global North and Global South cities. 'GNc' represents the Global North cities and 'GSc' represents the Global South cities. Box plots represent the interquartile range (IQR) as the box, median as a horizontal line within the box, mean as a point within the box, and 1.5× IQR as the whiskers. Outliers are omitted for clarity. (b) Differences in heat exposure index (HEI) between the global North and South. Heat exposure levels of global North and South cities are represented in red bar graph and blue bar graph, respectively, when considering urbanization-induced warming (real scenario). Heat exposure levels of global North and South cities without considering urbanization-induced warming (hypothetical scenario) are shown in grey bar graph. Error bars indicate standard deviation. The red and black dots indicate the average HEI difference between the global North and global South cities under the real and hypothetical scenarios, respectively.

Supplementary References

1 Zhang, T. *et al.* A global dataset of daily maximum and minimum near-surface air temperature at 1 km resolution over land (2003–2020). *Earth Syst. Sci. Data* **14**, 5637-5649 (2022).

2 Du, H. *et al.* Contrasting Trends and Drivers of Global Surface and Canopy Urban Heat Islands. *Geophys. Res. Lett.* **50**, e2023GL104661 (2023).

3 Zhang, T., Zhou, Y., Zhu, Z., Li, X. & Asrar, G. R. A global seamless 1 km resolution daily land surface temperature dataset (2003–2020). *Earth Syst. Sci. Data* **14**, 651-664 (2022).